Large refractive index enhancement in $PbTe/Pb_{1-x}Eu_xTe$ multiquantum-well structures

Shu Yuan, H. Krenn, G. Springholz, and G. Bauer
Institut für Halbleiterphysik, Universität Linz, A-4040 Linz, Austria

M. Kriechbaum
Institut für Theoretische Physik, Universität Graz, A-8010 Graz, Austria

(Received 24 August 1992; accepted for publication 1 December 1992)

Optical interband absorption between confined carrier states is studied in $PbTe/Pb_{1-x}Eu_xTe$ multiple quantum wells (MQWs). The frequency dependence of the refractive index is calculated by the Kramers–Kronig transformation of the absorption coefficient of the MQWs. It is shown that the observed interference fringes in mid-infrared transmission can only be accounted for if the enhancement of the refractive index $\eta(\omega)$ at the interband transition energies which follow from the Kramers–Kronig transformation are taken into account. These changes in η are as large as 19% (at $T=77$ K) and are thus relevant for the design and fabrication of mid-infrared QW lasers.

$PbTe/Pb_{1-x}Eu_xTe$ heterostructures are of interest for the fabrication of tunable diode lasers in the mid-infrared range (3–6.5 μm). Recently, Feit *et al.*[1] reported the highest cw operating temperature (203 K) for such mid-infrared lasers using a buried heterostructure concept. Previously, Partin *et al.*[2] had achieved up to 175 K cw operation using a side optical cavity quantum-well (QW) structure. These authors have stressed the importance of the waveguide properties for high-temperature operation, without having determined the refractive index variation across the QW structure.

It is well known that the refractive index exhibits remarkable changes at the fundamental absorption edge of bulk materials which was investigated by Stern[3] for III-V compounds and by Zemel *et al.*[4] for the narrow-gap lead salts, where the band nonparabolicity affects absorption and consequently the refractive index $\eta(\omega)$. It was shown that in GaAs/AlAs quantum wells (QWs) the enhancement of $\eta(\omega)$ close to interband resonances depends on the well and barrier thicknesses and barrier composition.[5,6] For these QWs the highest reported changes of η are of the order of 5% or smaller.[5,7] Furthermore electric fields influence the refractive index of QWs, which is important for electro-optic device applications.[8,9]

In this letter, we show that the dependence of the refractive index on the frequency exhibits pronounced maxima with $\Delta\eta/\eta$ as high as 19% close to the interband transitions between confined hole and electron states in $PbTe/Pb_{1-x}Eu_xTe$ multiquantum-well (MQW) structures. In addition, we demonstrate the necessity to take these variations of refractive index into account to explain quantitatively the optical transmission spectra of $PbTe/Pb_{1-x}Eu_xTe$ MQWs. In contrast to GaAs/GaAlAs MQWs, excitonic contributions to $\Delta\eta$ are practically absent in the lead compounds because of their huge dielectric constants.[10]

The $PbTe/Pb_{1-x}Eu_xTe$ MQWs were grown by molecular-beam epitaxy (MBE) on cleaved BaF_2 substrates.[11] As a buffer layer, $Pb_{1-x}Eu_xTe$ with a thickness of about 5 μm was deposited. In the samples studied, the well widths range from 62 to 118 Å and barrier widths from 486 to 648 Å, i.e., chosen to be much wider than the wells. The structural properties were checked by *in situ* reflection high-energy electron diffraction (RHEED) and by high-resolution x-ray diffraction.

In Fig. 1 the transmission spectrum for a typical sample (MQW No. 151) normalized to the transmission of the BaF_2 substrate is shown. The sample parameters of MQW No. 151 are: $d_w=62$ Å, $d_b=621$ Å, containing 46 periods, $d_{\text{buffer}}=5.32$ μm, and an Eu content of $x=2.6\%$. The mid-infrared transmission spectra were measured at $T=5$ and 77 K in the frequency range 800–4000 cm^{-1}.

Since the BaF_2 substrate is essentially transparent in this frequency range, the absorption is due to the $Pb_{1-x}Eu_xTe$ buffer layer and barrier layers, as well as due to the interband transitions between hole and electron subbands in the PbTe wells. The fringes in the transmission spectrum arise from multiple reflections and interference effects in the whole multilayer stack including the buffer. The main changes in the optical constants occur at the sample-air interface and at the interface to the BaF_2 substrate. The drastic steplike changes in the transmission signal are due to absorption involving the two-dimensional (2D) confined states in the PbTe wells. Similar observations were made by Ishida *et al.*[12] in a previous study. For the calculation of the transmission, the optical constants of the $Pb_{1-x}Eu_xTe$ buffer and barrier layers are needed. These were determined independently from a $Pb_{1-x}Eu_xTe$ reference sample. For the PbTe QWs we assume a perfect 2D system, i.e., we neglect the penetration of the carrier wave functions into the $Pb_{1-x}Eu_xTe$ barrier layers. The extinction coefficient in the QWs, taking level broadening into account, is then given by[13,14]

$$\kappa(\hbar\omega)=\sum_j A_j\left[\frac{\pi}{2}+\arctan\left(\frac{\hbar\omega-E_j}{\Gamma_j}\right)\right]\frac{1}{(\hbar\omega)^2}, \qquad (1)$$

where E_j denotes the interband transition energies between the confined states in the valence band (VB) and in the conduction band (CB) of the PbTe wells, Γ_j is a broadening parameter, j is the interband transition index, and $\hbar\omega$ is

 0003-6951/93/080885-03$06.00

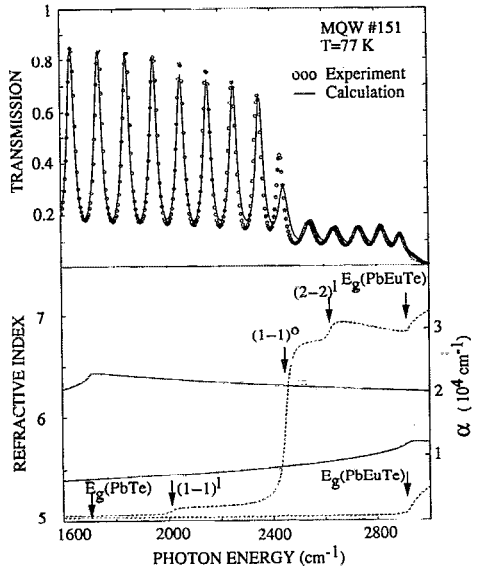

FIG. 1. Upper panel: transmission PbTe/$Pb_{1-x}Eu_xTe$ MQW sample with PbTe well widths of 62 Å and 46 periods, at $T=77$ K. Circles: experimental data; full lines: calculated data. Lower panel: absorption coefficient (dashed lines) in the QWs and in the $Pb_{1-x}Eu_xTe$ buffer and barrier layers. Interband transitions are indicated. Also shown are the refractive indices (full lines) of bulklike PbTe and $Pb_{1-x}Eu_xTe$ used for the calculation of the transmission as determined from single epitaxial layers.

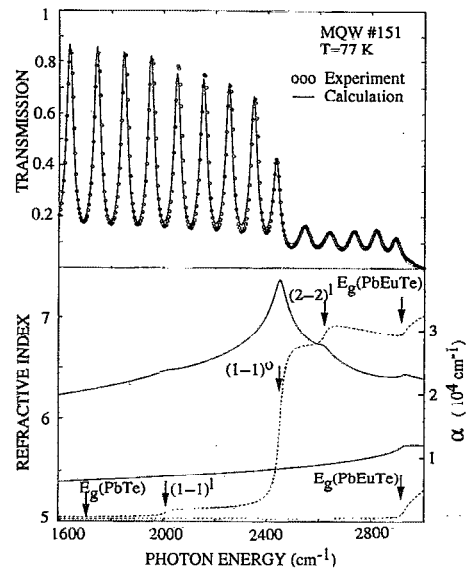

FIG. 2. Upper panel as Fig. 1, but considering the changes of refractive index due to interband absorptions between confined carrier states in the PbTe wells (full lines) as shown in the lower panel, calculated by Kramers–Kronig transformation from the absorption coefficient (dashed lines).

the photon energy. Since the growth is along [111] direction, two subband systems occur. One is associated with the valleys at the L point of the Brillouin zone along the [111] axis (l), which have circles as surfaces of constant energy in the k_x, k_y plane. The other three valleys with their main axes oriented obliquely (o) with respect to the [111] growth direction give rise to three ellipses as surfaces of constant energy in the 2D case. Consequently, the prefactor A_j which depends both on the 2D joint density of states as well as the transition matrix elements is different for transitions involving subbands of the longitudinal (l) and oblique (o) valleys:

$$A_j^{(l)}=\frac{e^2E_gP_\perp^2/P_\perp^2}{8\eta\epsilon_0\pi d_w} \tag{2a}$$

and

$$A_j^{(o)}=\frac{e^2g_vE_g(\frac{5}{9}+\frac{4}{9}P_\parallel^2/P_\perp^2)}{8\eta\epsilon_0\pi d_w}[\tfrac{1}{3}\sqrt{1+8P_\parallel^2/P_t^2}]^{-1} \tag{2b}$$

where E_g is the energy gap of PbTe, g_v ($=3$) is the oblique valley degeneracy index, $P_\perp$ and $P_\parallel$ are the transverse and longitudinal interband momentum matrix elements,[15] and d_w is the well width. For the fit of the experimental transmission data, the interband transition energies E_j and their broadenings Γ_j were used as fit parameters.

The corresponding variation of the absorption coefficient $\alpha(\omega)=4\pi\kappa(\omega)/\lambda$ versus photon energy is shown in Fig. 1, lower panel. The step in $\alpha(\omega)$ for the oblique valley interband transition $(1\rightarrow1)^o$ is by a factor of about 5 larger than those for the longitudinal valley transitions $(1\rightarrow1)^l$, $(2\rightarrow2)^l$ because of the threefold degeneracy, the differences in joint density of states masses, and in the transition-matrix element. However, the Γ_j were varied from 0.5 to 2 meV for these transitions to improve the overall fit. Also in the lower panel, the dependence of $\eta(\omega)$ is shown for bulk PbTe and $Pb_{1-x}Eu_xTe$ ($x=0.026$), which were experimentally determined from bulklike epitaxial layers.

The calculation of the transmission for the multilayer structure is based on $\alpha(\omega)$ and $\eta(\omega)$ for each of the PbTe and the $Pb_{1-x}Eu_xTe$ layers with properly matched electromagnetic fields at all interfaces in the sequence of layers using the transfer-matrix method.[16,17] The calculated transmission reproduces the main features of the measured data (see Fig. 1). However, in particular close to the $i=1$ (VB)$\rightarrow i=1$ (CB) transition in the oblique (o) subband ladder, the position of the interference fringes does not coincide with the measured values. Since the extinction coefficient $\kappa(\omega)$ and the refractive index $\eta(\omega)$ are related via the Kramers–Kronig relationship (KKR),

$$\eta(\omega)=\eta_\infty+\frac{1}{\pi}P\int_{-\infty}^{\infty}\frac{\kappa(\omega')-\kappa(\infty)}{\omega'-\omega}d\omega', \tag{3}$$

one can expect that especially in the IV-VI QWs in the 2D case, interband transitions will lead to substantial changes in $\eta(\omega)$. This is actually the case as shown in Fig. 2, where $\eta(\omega)$ has been calculated from $\kappa(\omega)$ according to Eq. (3), where the error due to the finite frequency range in KKR is less than 3%. At the frequencies where $\alpha(\omega)$ exhibits a steplike increase, $\eta(\omega)$ shows maxima. The stronger the changes in $\alpha(\omega)$, the more pronounced are the peaks in $\eta(\omega)$. For the $(1\rightarrow1)^o$ transition the increase of $\eta(\omega)$ is as large as 19% with respect to bulk PbTe at 2450 cm^{-1} (see Figs. 1 and 2). Using the calculated $\eta(\omega)$ for the PbTe well, and the experimental data for $\eta(\omega)$ for the $Pb_{1-x}Eu_xTe$ buffer and barrier layers, the theoretical trans-

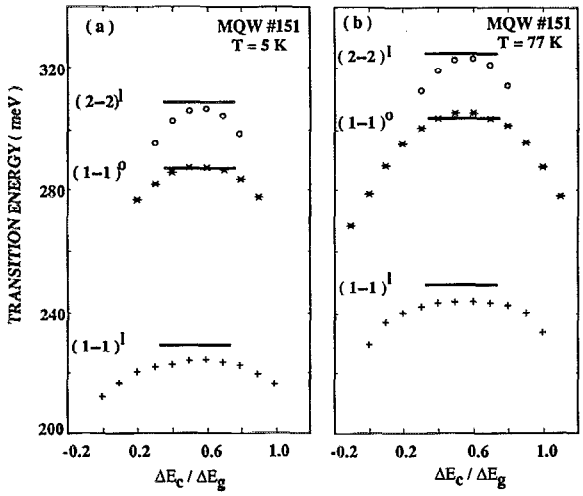

FIG. 3. Calculated interband transition energies for PbTe/$Pb_{1-x}Eu_xTe$ MQW sample for transitions involving longitudinal (l) and oblique (o) valleys for T=5 K (a) and T=77 K (b) as a function of normalized offset $\Delta E_c/\Delta E_g$. Experimentally observed transition energies are represented by straight lines.

mission spectra are in much better agreement with the experimental data (Fig. 2). In particular, the positions of the transmission extrema which are sensitive to the dispersion of $\eta(\omega)$ are well reproduced. The accuracy of the determination of η is better than 3% close to its maximum value at 2450 cm^{-1}. This was estimated from the corresponding calculated shift of the transmission by 3 cm^{-1} away from its experimental value which is easily observable.

In order to further analyze the data, the interband transition energies between confined states in the CB and the VB of the PbTe wells are calculated. For that purpose, an envelope function approximation (EFA) formalism is used for the IV-VI QWs,[18] with PbTe and PbEuTe band parameters as given in Ref. 15. Since for the band offsets in the PbTe/$Pb_{1-x}Eu_xTe$ system different values of $\Delta E_c/\Delta E_g$ =0.5–0.1 have been reported[2,12,19,20] (ΔE_c conduction-band offset, ΔE_g energy-gap difference), the QW interband transition energies were calculated for a range of different offset values.

The [111] QW geometry is helpful for the determination of the band offset since two sets of subbands occur. In our experiment, three individual transitions were observed. Among them, the $(2\rightarrow 2)^l$ transition is most sensitive to the band offset. In Fig. 3, the theoretical transition energies for different offset values are compared to the experimentally observed ones. The envelope part in the transition-matrix elements $|\langle\chi_i^c(z)^{l,o}|\chi_i^v(z)^{l,o}\rangle|^2$, where c, v denote CB and VB, respectively, depends quite remarkably on the offset for the $(2\rightarrow 2)^l$ transition and decreases by a factor of 10 outside the region $\Delta E_c/\Delta E_g=0.55\pm0.2$. Consequently, we conclude both from the transition energies as well as from their oscillator strengths, that the band offset in PbTe/$Pb_{1-x}Eu_xTe$ is quite symmetric, at least for low Eu contents ($x<5\%$). The EFA calculations show that for the relatively wide $Pb_{1-x}Eu_xTe$ barriers and for an offset of $\Delta E_c/\Delta E_g=0.55$, the penetration of the carrier wave functions into the barriers is comparatively small, which justifies the validity of the calculation of $\alpha(\omega)$ as described above except for frequencies close to the highest lying $(2\rightarrow 2)^l$ transition.

In conclusion, we have shown that in PbTe/$Pb_{1-x}Eu_xTe$ MQWs the refractive index changes considerably at photon energies close to the interband transitions between confined states. With respect to bulk PbTe, η increases up to 19% at interband transitions between confined states involving the oblique valleys. This fact is important for the optical confinement of radiation in mid-infrared QW lasers. From the comparison of the observed transition energies and their oscillator strengths with the calculated ones, we conclude that the band offset in the PbTe/$Pb_{1-x}Eu_xTe$ system (for $x<5\%$) is quite symmetric with $\Delta E_c/\Delta E_g=0.55\pm0.2$.

This work was supported by Fonds zu Förderung der Wissenschaftlichen Forschung, Vienna, Project No. 8250. S. Y. acknowledges support by ÖAD. We thank M. Seto for helpful discussions.

[1] Z. Feit, D. Kostyk, R. J. Woods, and P. Mak, Appl. Phys. Lett. **58**, 343 (1991).
[2] D. L. Partin, IEEE J. Quantum Electron. **QE-24**, 1716 (1988).
[3] F. Stern, Phys. Rev. **133**, A1653 (1964).
[4] J. N. Zemel, J. D. Jensen, and R. B. Schoolar, Phys. Rev. **140**, A330 (1965).
[5] Y. Suzuki and H. Okamoto, J. Electron. Mater. **12**, 397 (1983).
[6] C. Weisbuch and B. Vinter, *Quantum Semiconductor Structures* (Academic, San Diego, 1991), p. 70.
[7] K. B. Kahn and J. Leburton, Appl. Phys. Lett. **47**, 508 (1985).
[8] S. Schmitt-Rink, D. S. Chemla, and D. A. B. Miller, Adv. Phys. **38**, 89 (1989).
[9] K. Nakamura, A. Shimizu, K. Fujii, M. Koshiba, and K. Hayata, IEEE J. Quantum Electron. **QE-28**, 1670 (1992).
[10] G. Bauer and H. Krenn, in *Handbook of Optical Constants*, ed. E. D. Palik (Academic, Orlando, FL, 1985), p. 535.
[11] G. Springholz and G. Bauer, Appl. Phys. Lett. **60**, 1600 (1992).
[12] A. Ishida, S. Matsuura, M. Mizuno, and H. Fujiyasu, Appl. Phys. Lett. **51**, 478 (1987).
[13] G. Bastard, *Waves Mechanics Applied to Semiconductor Heterostructures* (Editions de Physique, Paris, 1989), p. 13.
[14] H. S. Cho and P. R. Prucnal, Phys. Rev. B **39**, 11150 (1989).
[15] G. Bauer, H. Pascher, and W. Zawadzki, Semicond. Sci. Technol. **7**, 703 (1992).
[16] B. Harbecke, Appl. Phys. B **39**, 165 (1986).
[17] A. F. Terzis, X. C. Liu, A. Petrou, B. D. McCombe, M. Dutta, H. Shen, Doran D. Smith, M. W. Cole, M. Taysing-Lara, and P. G. Newman, J. Appl. Phys. **67**, 2501 (1990).
[18] M. Kriechbaum, Spring Ser. Solid State Sci. **63**, 120 (1984); IEEE J. Quantum Electron. **QE-24**, 1727 (1988).
[19] E. T. Heyen, M. Hagerott, A. V. Nurmikko, and D. L. Partin, Appl. Phys. Lett. **54**, 653 (1989).
[20] L. S. Kim, H. D. Drew, R. E. Doezema, J. P. Heremans, and D. L. Partin, Phys. Rev. B **35**, 251 (1989).